Organic Electronics 13 (2012) 975–979

Contents lists available at SciVerse ScienceDirect

Organic Electronics

journal homepage: www.elsevier.com/locate/orgel

CdSe-sensitized inorganic–organic heterojunction solar cells: The effect of molecular dipole interface modification and surface passivation

Yong Hui Lee [a,b,1], Sang Hyuk Im [a,1], Jeong Ah Chang [a], Jong-Heun Lee [b], Sang Il Seok [a,*]

[a] KRICT-EPFL Global Research Laboratory, Advanced Materials Division, Korea Research Institute of Chemical Technology, 141 Gajeong-ro, Yuseong-gu, Daejeon 305-600, Republic of Korea
[b] Department of Materials Science and Engineering, Korea University, Anam-Dong, Sungbuk-Gu, Seoul 136-713, Republic of Korea

ARTICLE INFO

Article history:
Received 4 December 2011
Received in revised form 3 February 2012
Accepted 11 February 2012
Available online 14 March 2012

Keywords:
Solar cells
CdSe-sensitized
Poly-3-hexylthiophene
Interface modification
Surface passivation

ABSTRACT

CdSe-sensitized heterojunction solar cells composed of mesoscopic TiO_2/CdSe/P3HT (poly-3-hexylthiophene) were constructed, and the negative molecular dipole of 4-methoxybenzenethiol (MBT) and the ZnS passivation layer were used as interface modifiers to improve device performance. Through the interface modification between TiO_2/CdSe and P3HT using MBT and by ZnS surface passivation, the power conversion efficiency of the modified solar cell was greatly enhanced from 1.02% to 1.62% under 1 sun illumination.

1. Introduction

Solar energy conversion systems have received considerable attention because solar energy is abundant, renewable, and clean. Conventional silicon solar cells would be placed by dye-sensitized solar cells (D-SSCs) [1] and bulk heterojunction-organic solar cells (BHJ-OSCs) [2], which are considered representative next-generation solar cells. D-SSCs are unique because they are composed of a mesoscopic photoanode, sensitizer, and hole transporting material, which serve as an electron conductor, light absorber, and redox electrolyte. The separate role of each component enables D-SSCs to maintain good performance because the possibility of recombination is very low. A considerable enhancement in device efficiency has been successfully demonstrated by the extremely enlarged interfacial area in both D-SSCs and BHJ-OSCs. Therefore, it is desirable to use morphologically pre-developed porous architecture to attain high device efficiency. In addition, the use of a solid-state hole conductor instead of a conventional liquid redox electrolyte can prevent potential electrolyte leakage and enable the fabrication of flexible devices. Accordingly, low-cost and highly efficient solar cells can be developed by combining the porous architecture of the electron conductor in D-SSCs and the solid-state hole conductor in BHJ-OSCs.

Inorganic semiconductors and quantum dots have been considered promising alternatives to conventional organic dyes owing to their unique properties such as a high extinction coefficient, intrinsically large dipole moment, convenient bandgap tunability, multiple exciton generation, and good stability [3]. Therefore, metal chalcogenides such as CdS(e) [4–7], PbS(e) [8–10], and Sb_2S_3 [11–15] have been used as inorganic semiconductor sensitizers. Recently, we reported on the fabrication of highly efficient Sb_2S_3-sensitized inorganic–organic heterojunction solar cells [11,12]. However, efficient solid-state CdSe-sensitized heterojunction solar cells have not been reported, despite the development of efficient liquid-type CdSe-sensitized photoelectrochemical solar cells [16] and the fact that

* Corresponding author. Fax: +82 42 861 4151.
E-mail address: seoksi@krict.re.kr (S.I. Seok).
[1] These two authors have equally contributed to this study.

1566-1199/$ - see front matter © 2012 Elsevier B.V. All rights reserved.
http://dx.doi.org/10.1016/j.orgel.2012.02.011

the bulk bandgap of CdSe is similar to that of Sb_2S_3. This might be attributed to the upset or insufficient difference in energy level between CdSe and TiO_2 to attain an efficient charge injection process.

Shalom et al. [17] suggested that a molecular dipole attached to an inorganic semiconductor surface can increase the energy levels toward the vacuum level, causing the electron injection to become more favorable. Chi et al. [18] recently reported that molecular dipole treatment is still effective in solid-state CdS/CdSe-co-sensitized solar cells composed of mesoscopic TiO_2/CdS-CdSe/spiro-MeOTAD (2,2′,7,7′-tetrakis (*N*,*N*-di-*p*-methoxyphenylamine)-9,9′-spirobifluorene). Through molecular dipole treatment using an inorganic semiconductor sensitizer and TiO_2 surface passivation, they could attain a 0.88% power conversion efficiency at 1 sun illumination (AM 1.5G 100 mW/cm^2). Unlike the wide bandgap spiro-MeOTAD hole conductor, P3HT (poly-3-hexylthiophene) can absorb visible light and generate charge carriers. It has been reported that the generated charge carriers in the P3HT donor can be transported to the CdSe acceptor in hybrid solar cells [19] and transported to TiO_2 through a CdS intermediate [20]. To improve the device performance of CdSe-sensitized solar cells, here, we fabricated CdSe-sensitized heterojunction solar cells composed of mesoscopic TiO_2/CdSe/P3HT as an electron conductor/inorganic semiconductor sensitizer/hole conducting dye layer and treated the CdSe surface with a molecular dipole.

2. Experimental

2.1. Device fabrication

A 100-nm-thick dense TiO_2 blocking layer (bl-TiO_2) was deposited on an F-doped SnO_2 (FTO, Pilkington, TEC 8) glass substrate by spray pyrolysis deposition of 20 mM of titanium diisopropoxide bis(acetylacetonate) (Aldrich) solution at 450 °C to prevent the hole conductor from being in direct contact with the FTO substrate. A 1-μm-thick mesoscopic TiO_2 layer (particle size = ~50 nm, anatase) [13,21] was then screen printed onto a bl-TiO_2/FTO substrate and heat-treated at 500 °C for 30 min in air. It should be noted that the transparent FTO glass substrate was cleaned ultrasonically in successive baths in acetone and ethanol and then dried under airflow before use. The CdSe sensitizer was prepared by the successive ionic layer adsorption and reaction (SILAR) process. For deposition, TiO_2 films were successively immersed into 0.03 M $Cd(NO_3)_2$ in ethanol and then into 0.03 M Se^{2-} precursor for 30 s each [13,22]. After cation dipping, the film was washed with ethanol, dried with an air blower, and dipped in anion precursor. This SILAR process was repeated 8 (CdSe-8), 10 (CdSe-10), and 12 (CdSe-12) times. Selenium precursor [23] was prepared by reducing SeO_2 with $NaBH_4$ in ethanol under an Ar atmosphere. All processes were carried out in an Ar-purged glove box. For negative molecular dipole interface modification, 1 mL of 0.1 M 4-methoxybenzenethiol (MBT) solution in ethanol was dropped onto mesoscopic CdSe/TiO_2 films and spin-coated for 30 s at 3000 rpm. For ZnS surface passivation, the ZnS layer was formed on a CdSe/TiO_2(/MBT) film by successive dipping into 0.05 M $Zn(NO_3)_2$ and 0.05 M Na_2S aqueous solution via 1 cycle of the SILAR process. The P3HT (98% regioregular, Rieke) solution (15 mg/1 mL dichlorobenzene) was spincoated at 2500 rpm for 60 s. PEDOT:PSS (AI 4083, Clevios) in methanol (1/2 v/v) was then spincoated at 2500 rpm for 60 s and dried at 90 °C for 30 min in a vacuum oven. Finally, a Au counter electrode was deposited by thermal evaporation. The active area of the device was fixed at 0.16 cm^2.

2.2. Device characterization

The current density–voltage (*J*–*V*) characteristics of the cells were measured under 100 mW/cm^2 illumination using a solar simulator (Newport Co. Oriel Class A, 91195A) with a Keithley 2420 Source Meter® and a calibrated Si-reference cell (certified by NREL). The external quantum efficiency (EQE) was measured using a fully computerized home-designed system consisting of a light source (Newport 300 W Xenon lamp 66902) aligned with a monochromator (Newport Cornerstone™ 260) and a multimeter (Keithley 2001). *J*–*V* characteristics of the cells were measured using a metal mask of 0.16 cm^2.

3. Results and discussion

The schematic energy band diagram of the CdSe-sensitized inorganic–organic heterojunction solar cell is shown in Fig. 1(a). The CdSe nanoparticles generate electron–hole pairs by illuminated external light, and the generated electrons (holes) are injected into TiO_2 (P3HT). At the same time, the P3HT also absorbs the light and generates electron–hole pairs; the electrons from these pairs can be cascade-transferred to TiO_2 through the CdSe intermediate. It should be noted that P3HT has the dual function of hole conductor and light absorber; thus, it was named a hole conducting dye. Generally, the sizes of the CdSe nanoparticles produced by the SILAR process are polydispersed; consequently, a diverse energy bandgap associated with the CdSe sensitizer will coexist in the device, as shown in Fig. 1(a). The smaller CdSe nanoparticles can more energetically inject electrons into TiO_2 than the larger ones owing to the quantum size effect. Therefore, a negative molecular dipole interface treatment at the CdSe/P3HT interface should be desirable to more energetically inject electrons from CdSe to TiO_2, The SEM cross-sectional image of the CdSe-sensitized heterojunction solar cell shown in Fig. 1(b) demonstrates that the thickness of the mesoscopic TiO_2 electron conductor is ~1 μm. It should be noted that, unlike in liquid photoelectrochemical solar cells, the thickness of the mesoscopic TiO_2 layer is limited by the pore-filling problem associated with hole transporting materials in solid-state solar cells. Therefore, we used ~1-μm-thick TiO_2 film that had been previously confirmed not to have a pore-filling problem [13]. A typical TEM image of CdSe nanoparticles deposited on mesoscopic TiO_2 film is shown in Fig. 1(c). This image clearly indicates that most of the surfaces of the TiO_2 nanoparticles are well covered by CdSe nanoparticles. The TiO_2 (~50 nm) and CdSe (~5 nm)

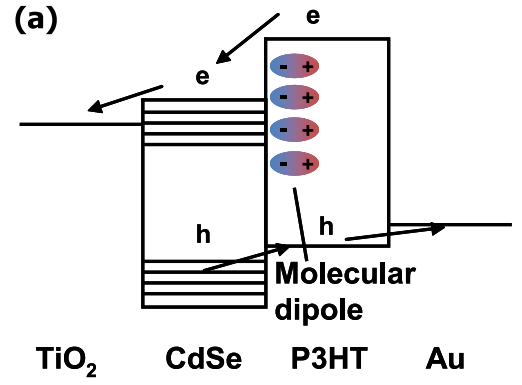

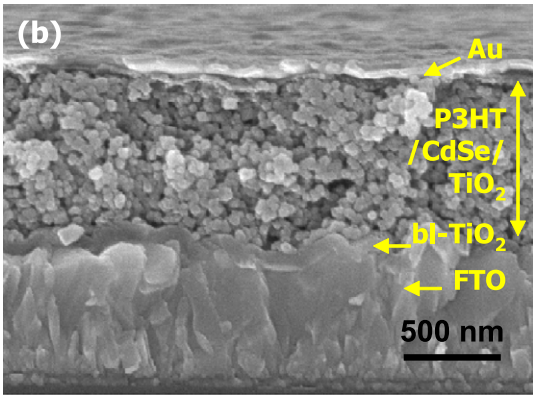

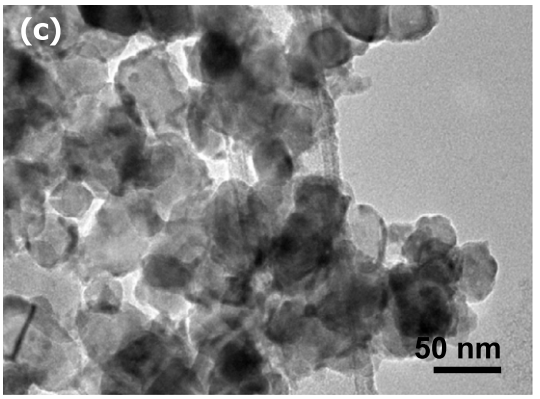

Fig. 1. (a) Schematic illustration of energy band diagram of CdSe-sensitized heterojunction solar cell, (b) cross-sectional SEM image, and (c) TEM image of CdSe deposited on mesoscopic TiO_2 electrode.

nanoparticles can be recognized on the TEM image based on their distinctive size.

Fig. 2(a) shows the UV–Vis transmission spectra of CdSe deposited on a mesoscopic TiO_2 film with the number of times the SILAR process is repeated (SILAR cycles). As the number of SILAR cycles increases, the absorption is intensified and red-shifted owing to the increased concentration and size of the deposited CdSe nanoparticles. The photographs in the inset of Fig. 2(a) clearly indicate that stronger absorption is associated with increased number of SILAR cycles. The photocurrent density–voltage (*J–V*) curves and

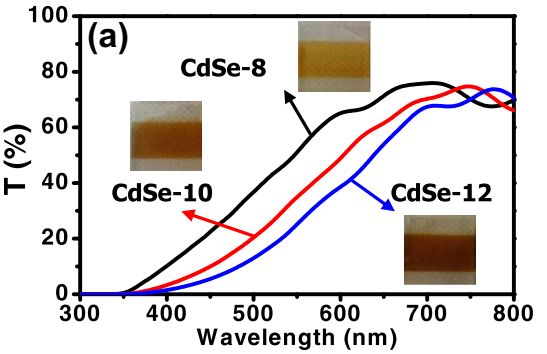

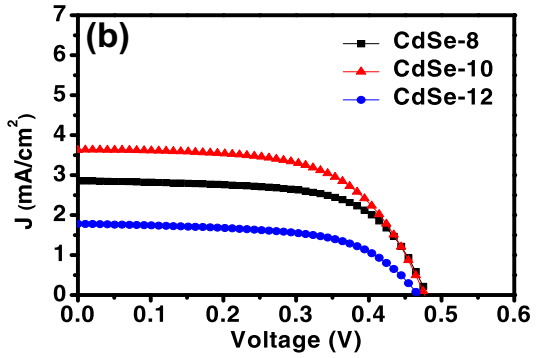

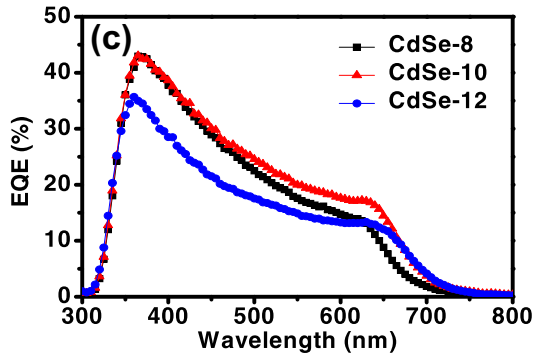

Fig. 2. (a) UV–Vis transmission spectra of CdSe deposited on mesoscopic TiO_2 film according to the number of SILAR cycles: inset = photograph, (b) *J–V* curves, and (c) EQE spectra of CdSe-sensitized heterojunction solar cells.

the number of SILAR cycles are shown in Fig. 2(b). The performance of all devices is summarized in Table 1. The *J–V* curves indicate that the optimal device performance (1.09% at 1 sun illumination) was obtained for the CdSe-10 sample subjected to 10 cycles of SILAR. Furthermore, the results indicate that a thicker deposit of CdSe

Table 1
Summary of device performance with the number of SILAR cycles.

	J_{sc} (mA/cm^2)	V_{oc} (V)	F.F (%)	η (%)
CdSe-8	2.9	0.47	64.0	0.94
CdSe-10	3.6	0.47	60.7	1.09
CdSe-12	1.8	0.46	59.7	0.52

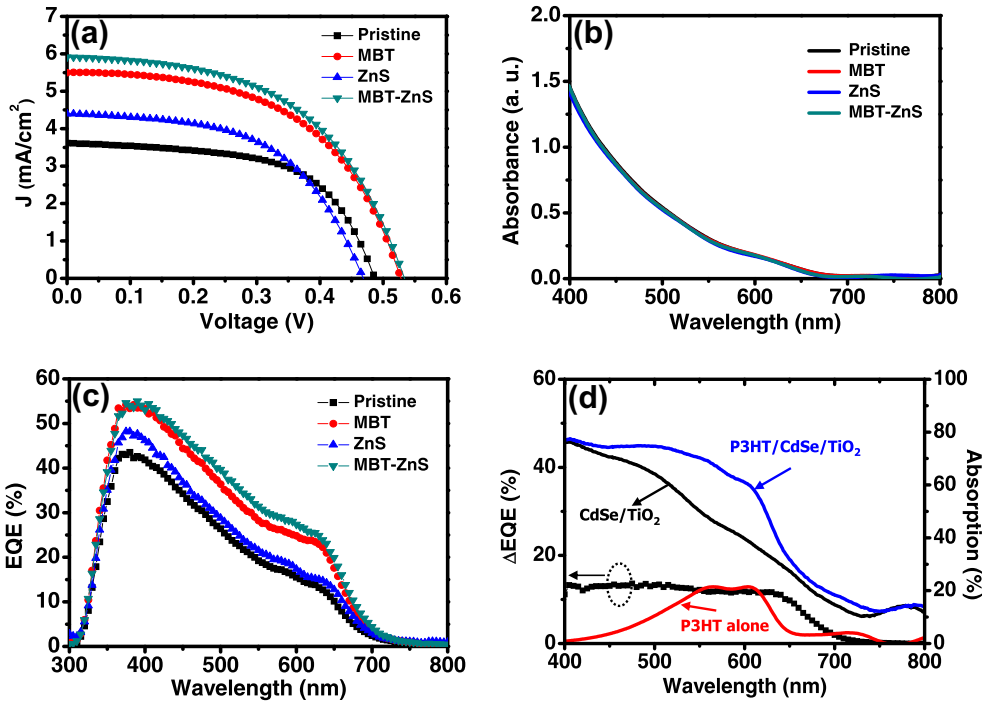

Fig. 3. (a) *J–V* curves, (b) UV–Vis absorption spectra, (c) EQE spectra of CdSe-sensitized heterojunction solar cells with different interface modifications, and (d) absorption spectra of P3HT/CdSe/TiO_2, CdSe/TiO_2, and P3HT alone and ΔEQE of MBT-ZS and pristine device in (c).

(CdSe-12: power conversion efficiency = 0.52%) degraded the power conversion efficiency owing to significant degradation of the short circuit current density (J_{sc}). The serious degradation of J_{sc} might be attributed to the thickly aggregated CdSe nanoparticles or pore-filling problem associated with P3HT and the narrow pore volume. Significant degradation of performance in thicker CdSe samples (CdSe-12) was also observed when polysulfide was used as the hole conductor instead of P3HT (data not shown). Hence, the thickly aggregated CdSe nanoparticles might seriously deteriorate the device performance. The external quantum efficiency (EQE) spectra of each device shown in Fig. 2(c) were consistent with the J_{sc} of each cell. As the number of SILAR cycles increased, the optimal EQE value was achieved at longer wavelengths; this indicates the formation of larger CdSe nanoparticles. The EQE is related to light harvesting, charge injection, and charge collection efficiency. Accordingly, the degradation of EQE in thickly aggregated CdSe samples (CdSe-12) is a result of degraded charge injection or collection efficiency, even though the light harvesting efficiency increases owing to increased absorption by the thicker CdSe nanoparticles. By repeating the SILAR process, we optimized the device performance of the CdSe-10 sample under the present experimental conditions. Hereafter, we considered the CdSe-10 sample to be a pristine device for further comparison to examine the effects of interface modification.

To check the effects of interface modification on the device performance, we measured the *J–V* curves of model devices with modified interfaces as shown in Fig. 3(a). All device performances are summarized in Table 2. For this model experiment, we prepared samples with the same light harvesting efficiency by depositing CdSe on a mesoscopic TiO_2 film under the same experimental conditions. The exact match of the UV–Vis absorption spectra of all samples shown in Fig. 3(b) confirms that the light harvesting by all devices was the same. The similar device performance of the newly fabricated pristine sample (η = 1.02%) as the CdSe-10 device (η = 1.09%) in Fig. 2(b) confirms that this device is reproducible, and that the deposited concentration of CdSe is almost the same because the short circuit current densities of both pristine samples are same to 3.6 mA/cm^2. As expected, the MBT-treated device exhibits considerably enhanced device performance (η = 1.52%). The improved device efficiency is caused by the improved short circuit current density (3.6 → 5.5 mA/cm^2) and open circuit voltage (0.48 → 0.53 V). Overall, a 53% improvement in short circuit current density (J_{sc}) in response to interface modification with the negative molecular dipole was observed. It was reported [16,17] that the MBT monolayer attached to the surface of CdSe via thiol group (SH–) induces a negative dipole field on the CdSe surface, which is anticipated to result in an upward shift of the

Table 2
Summary of device performance with different interface modifications.

	J_{sc} (mA/cm^2)	V_{oc} (V)	F.F (%)	η (%)
Pristine	3.6	0.48	59.3	1.02
MBT	5.5	0.53	53.6	1.52
ZnS	4.4	0.46	54.5	1.09
MBT-ZnS	5.9	0.54	53.5	1.62

CdSe energy levels. Therefore, MBT-treatment can lead to the more energetic injection of charge carriers from the CdSe sensitizer or the improved cascade charge transfer from P3HT to TiO_2 through the CdSe intermediate. In addition, the enhancement of V_{oc} by the molecular dipole modification can be related with reduced recombination between TiO_2 and P3HT [18].

The formation of a ZnS passivation layer at the (TiO_2/CdSe)/P3HT interface leads to a slight improvement in power conversion efficiency ($\eta = 1.02 \rightarrow 1.09\%$) caused by the improved J_{sc} from 3.6 to 4.4 mA/cm^2. The sequential interface modification by MBT and ZnS (MBT-ZnS) exhibits an optimal power conversion efficiency of 1.62% owing to the improved charge transfer/transport at the TiO_2/CdSe/P3HT interface and passivation at the TiO_2/P3HT interface. As shown in Fig. 3(c), the EQE spectra of each model device matched the short circuit current density of each cell well. The improved EQE values confirm that the interface modification results in improved charge injection or collection efficiency because the light harvest efficiency is constant. However, it is still not clear if the improved device performance is mainly derived from more energetic charge injection from CdSe to TiO_2 or the improved cascade charge transfer/transport from P3HT to TiO_2 through the CdSe intermediate. The absorption spectra of CdSe/TiO_2 and P3HT/CdSe/TiO_2 were measured to compare the shape and portion of each component (Fig. 3(d)). The CdSe deposited on mesoscopic TiO_2 absorbed light at wavelengths up to 750 nm. The absorption by only P3HT in the device was estimated based on the difference in the absorption spectra of P3HT/CdSe/TiO_2 and CdSe/TiO_2. The absorption spectrum of P3HT indicates that absorption begins at 650 nm, and that strong absorption occurs at 560–600 nm. Assuming that the charge carriers generated by P3HT are efficiently transported to TiO_2 through the CdSe intermediate by negative molecular dipole interface modification, the shape of the improved EQE spectrum will be matched to the absorption spectrum of P3HT. However, as shown in Fig. 3(d), the shape of the improved EQE spectrum in response to interface modification does not match the P3HT absorption spectrum. Therefore, the considerable enhancement in device performance in response to interface modification might primarily be derived from the improved charge injection from CdSe to TiO_2.

4. Conclusion

We constructed CdSe-sensitized heterojunction solar cells composed of mesoscopic TiO_2/CdSe/P3HT (poly-3-hexylthiophene) as an electron conductor/sensitizer/hole conducting dye. To improve the device performance, we modified the interface of TiO_2/CdSe/P3HT with MBT as a negative molecular dipole and ZnS as a passivation layer. Through interface modification, we improved the power conversion efficiency of the modified solar cell by 59% (from 1.02% to 1.62% under 1 sun illumination) when compared to that of an unmodified pristine device. The improvement in performance induced by the interface modification might affect the energetic injection of electrons from CdSe to TiO_2.

Acknowledgments

This study was supported by the Global Research Laboratory (GRL) Program and the Global Frontier R&D Program on Center for Multiscale Energy System funded by the National Research Foundation under the Ministry of Education, Science and Technology of Korea, and by a grant from the KRICT 2020 Program for Future Technology of the Korea Research Institute of Chemical Technology (KRICT), Republic of Korea.

References

[1] B. O'Regan, M. Grätzel, Nature 353 (1991) 737.
[2] G. Yu, J. Gao, J.C. Hummelen, F. Wudl, A.J. Heeger, Science 270 (1995) 1789.
[3] A.J. Nozik, Chem. Phys. Lett. 457 (2008) 3.
[4] Y.-L. Lee, Y.-S. Lo, Adv. Funct. Mater. 19 (2009) 604.
[5] S.H. Im, Y.H. Lee, S.I. Seok, Electrochim. Acta 55 (2010) 5665.
[6] T. Zeng, H. Tao, X. Sui, X. Zhou, X. Zhao, Chem. Phys. Lett. 508 (2011) 130.
[7] S.H. Im, Y.H. Lee, S.I. Seok, S.W. Kim, Langmuir 26 (2010) 18576.
[8] H.J. Lee, P. Chen, S.-J. Moon, F. Sauvage, K. Sivula, T. Bessho, D.R. Gamelin, P. Comte, S.M. Zakeeruddin, S.I. Seok, M. Grätzel, Md.K. Nazeeruddin, Langmuir 25 (2009) 7602.
[9] S.H. Im, H.-J. Kim, S.W. Kim, S.I. Seok, Energy Environ. Sci. 4 (2011) 4181.
[10] S.H. Im, J.A. Chang, S.W. Kim, S.-W. Kim, S.I. Seok, Org. Electron. 11 (2010) 696.
[11] Y. Itzhaik, O. Niitsoo, M. Page, G. Hodes, J. Phys. Chem. C 113 (2009) 4254.
[12] S.-J. Moon, Y. Itzhaik, J.-H. Yum, S.M. Zakeeruddin, G. Hodes, M. Grätzel, J. Phys. Chem. Lett. 1 (2010) 1524.
[13] J.A. Chang, J.H. Rhee, S.H. Im, Y.H. Lee, H.-J. Kim, S.I. Seok, Md.K. Nazeeruddin, M. Grätzel, Nano Lett. 10 (2010) 2609.
[14] S.H. Im, C.-S. Lim, J.A. Chang, Y.H. Lee, N. Maiti, H.J. Kim, Md.K. Nazeeruddin, M. Grätzel, S.I. Seok, Nano Lett. 11 (2011) 4789.
[15] S.H. Im, H.J. Kim, C.-S. Lim, S.I. Seok, Energy Environ. Sci. 4 (2011) 2799.
[16] X.-Y. Yu, J.-Y. Liao, K.-Q. Qiu, D.-B. Kuang, C.-Y. Su, ACS Nano doi:10.1021/nn203375g.
[17] M. Shalom, S. Rühle, I. Hod, S. Yahav, A. Zaban, J. Am. Chem. Soc. 131 (2009) 9876.
[18] C.-F. Chi, P. Chen, Y.-L. Lee, I.-P. Liu, S.-C. Chou, X.-Li. Zhang, U. Bach, J. Mater. Chem. 21 (2011) 17534.
[19] W.H. Huynh, J.J. Dittmer, A.P. Alivistos, Science 295 (2002) 2425.
[20] J. Qian, Q.-S. Liu, G. Li, K.-J. Jiang, L.-M. Yang, Y. Song, Chem. Commun. 47 (2011) 6461.
[21] I.C. Baek, M. Vithal, J.A. Chang, J.-H. Yum, Md.K. Nazeeruddin, M. Grätzel, Y.C. Chung, S.I. Seok, Electrochem. Commun. 11 (2009) 909.
[22] M.T.S. Nair, Y. Peña, J. Campos, V.M. García, P.K. Nair, J. Electrochem. Soc. 145 (1998) 2113.
[23] H.J. Lee, M. Wang, P. Chen, D.R. Gamelin, S.M. Zakeeruddin, M. Grätzel, Md.K. Nazeeruddin, Nano Lett. 9 (2009) 4221.